2016

Cadmium and Secondary Structure-dependent Function of a Degron in the Pca1p Cadmium Exporter

Nathan Smith
University of Nebraska-Lincoln

Wenzhong Wel
University of Nebraska at Lincoln

Miaoyun Zhao
University of Nebraska-Lincoln, zhaomiaoyun2001@gmail.com

Xiaojuan Quin
University of Nebraska - Lincoln

Javier Seravalli
University of Nebraska-Lincoln, jseravalli1@unl.edu

See next page for additional authors

THE JOURNAL OF BIOLOGICAL CHEMISTRY VOL. 291, NO. 23, pp. 12420–12431, June 3, 2016

Cadmium and Secondary Structure-dependent Function of a Degron in the Pca1p Cadmium Exporter*

Received for publication, March 1, 2016, and in revised form, April 5, 2016 Published, JBC Papers in Press, April 8, 2016, DOI 10.1074/jbc.M116.724930

Nathan Smith[‡], Wenzhong Wei[‡], Miaoyun Zhao[‡], Xiaojuan Qin[‡§], Javier Seravalli[‡], Heejeong Kim[‡], and Jaekwon Lee[‡1]

From the [‡]Department of Biochemistry and Redox Biology Center, University of Nebraska, Lincoln, Nebraska, 68588-0664 and the [§]College of Life and Environmental Sciences, Shanghai Normal University, Shanghai 200234, China

Protein turnover is a critical cellular process regulating biochemical pathways and destroying terminally misfolded or damaged proteins. Pca1p, a cadmium exporter in the yeast *Saccharomyces cerevisiae*, is rapidly degraded by the endoplasmic reticulum-associated degradation (ERAD) system via a cis-acting degron that exists at the 250–350 amino acid region of Pca1p and is transferable to other proteins to serve as a degradation signal. Cadmium stabilizes Pca1p in a manner dependent on the degron. This suggested that cadmium-mediated masking of the degron impedes its interaction with the molecular factors involved in the ERAD. The characteristics and mechanisms of action of the degron in Pca1p and most of those in other proteins however remain to be determined. The results presented here indicate that specific cysteine residues in a degron of Pca1p sense cadmium. An unbiased approach selecting non-functional degrons indicated a critical role of hydrophobic amino acids in the degron for its function. A secondary structure modeling predicted the formation of an amphipathic helix. Site-directed mutagenesis confirmed the functional significance of the hydrophobic patch. Last, hydrophobic amino acids in the degron- and cadmium-binding region affected the interaction of Pca1p with the Ssa1p molecular chaperone, which is involved in ERAD. These results reveal the mechanism of action of the degron, which might be useful for the identification and characterization of other degrons.

The regulation of a number of biochemical pathways relies on turnover control of specific proteins (1, 2). The protein homeostasis system also destroys terminally misfolded or damaged proteins to prevent their accumulation and aggregation (3, 4). In line with these vital roles, defects in proteostasis in association with genetic and epigenetic problems, cellular stress, and/or reduced cellular capacity are attributed to multiple diseases such as neurodegenerative diseases, cystic fibrosis, diabetes, and cancer (5–7).

Degradation of proteins in response to cellular cues should be specific, highly targeted, and dynamic. The conditional exposure of the degradation signals, degrons, could determine the recruitment of molecular factors involved in the degradation process (1, 8). Degrons are controlled through diverse mechanisms such as posttranslational modifications (*e.g.* hydroxylation, glycosylation, and phosphorylation), protein-protein interactions, and the binding of specific metabolites (9–13). Despite this conceptual frame and many examples displaying regulated turnover, only a few degrons have been identified and characterized. For instance, IκB phosphorylation or Cys residue modification of KEAP1 leads to their dissociation from NF-κB and NRF2, respectively, to stabilize these transcription regulators (12). Hydroxylation of specific proline residues within HIF-1 recruits an ubiquitin ligase complex (14). If degron is defined as a region of a protein that is transferrable to other proteins with the maintenance of its role for protein degradation, then the degron in the Matα2p transcription repressor in yeast has been relatively well characterized (1, 15). Dimerization of Matα2p with Mata1p hides the degron (16), indicating exposure control of a degron through protein multimerization. The degron in Matα2p forms an amphipathic helix, and the hydrophobic face of the helix appears to be the primary signal for recruiting degradation machinery (16). Similar characteristics were also found in a degron of mammalian SGK1 (17). Nevertheless, in most cases, the characteristics and regulatory mechanisms of degrons remain unknown.

Cells also degrade unassembled, misfolded, or damaged proteins to prevent their toxicity. Translational errors, protein denaturation, and damage by stressors such as heat, heavy metals, and defects in maturation, such as multimerization, glycosylation, or cofactor binding, all result in the production of proteins that are non-functional and prone to aggregation (18). For instance, the endoplasmic reticulum-associated degradation (ERAD)[2] system controls the quality of proteins that are first targeted to the lumen or membrane of the ER for distribution to different cellular compartments (19, 20). Maturation defects of secretory proteins result in their destruction by the ubiquitin/proteasome system within the cytosol. Several model substrates possessing mutations, such as CFTRΔF508, Cpy1*p, and Ste6*p, as well as non-mutated proteins, such as apolipoprotein B and Hmg2p, have been studied (18, 21–24). Although many different molecular factors involved in the process have been

* This work was supported by National Institutes of Health Grants ES16337 (to J. L.) and P30GM103335 (to the Nebraska Redox Biology Center). The authors declare that they have no conflicts of interest with the contents of this article. The content is solely the responsibility of the authors and does not necessarily represent the official views of the National Institutes of Health.

[1] To whom correspondence should be addressed: Dept. of Biochemistry and Redox Biology Center, University of Nebraska, Lincoln, NE 68588-0664. Tel.: 402-472-2658; E-mail: jlee7@unl.edu.

[2] The abbreviations used are: ERAD, endoplasmic reticulum-associated degradation; SC, synthetic complete; 3HA, triple hemagglutinin; 2Myc, double c-myc; TCEP, tris(2-carboxyethyl)phosphine; MT, metallothionein.

identified (25), the mechanistic details remain to be investigated.

Ubiquitin often acts as a "tag" for the regulatory degradation of proteins, and the proteasome is a major destination for the degradation of those proteins (2, 25–26). There is also mounting evidence for the role of Hsp70p chaperones in the degradation of proteins, including several ERAD substrates (18, 27–29), which can at least partially resolve how the substrates of degradation pathways are initially recognized.

We have documented that Pca1p in the yeast *Saccharomyces cerevisiae* is a cadmium-exporting P-type ATPase and contains a degron at the cytoplasmic N terminus (9, 30). The degron residing between the 250th and 350th amino acids of Pca1p is responsible for ERAD-mediated degradation of Pca1p and another protein fused with the sequence (9, 30). Cadmium in the culture medium rapidly up-regulates Pca1p via a degron-dependent mechanism (31). Given the seven Cys residues within the degron and the high affinity of cadmium for thiols (9), cadmium could directly bind to the degron as a mechanism of cadmium sensing and control of degron function. This ERAD-mediated expressional control of a cell surface protein by a cis-acting degron rather than misfolding or by an assembly defect illustrates an intriguing mechanism underlying protein turnover.

This study aimed to gain better insights into the characteristics and regulatory mechanisms of a degron in Pca1p. Our data suggest that direct cadmium sensing by specific Cys residues in a degron of Pca1p alters its secondary structure to limit the exposure of hydrophobic residues, which reduces binding of the degron with Ssa1p, a molecular chaperone involved in protein degradation.

Experimental Procedures

Yeast Strains and Growth Conditions—The BY4741 haploid *S. cerevisiae* strain (*MATa his3Δ1, leu2Δ0, met15Δ0, ura3Δ0*) and isogenic strains containing specific gene deletion, including *pdr5*Δ and *yor1*Δ, were obtained from Open Biosystems. The *ssa2,3,4*Δ, *ssa1–45,ssa2,3,4*Δ, and isogenic control WT strains (32) were provided by E. Craig (University of Wisconsin, Madison, WI). Cells were cultured in the synthetic complete (SC) medium (2% (w/v) dextrose, 0.2% (w/v) amino acid mixture, and 0.67% (w/v) yeast nitrogen base) lacking uracil for plasmid selection (SC-ura), YPD medium (1% (w/v) yeast extract, 2%(w/v) bacto-peptone, and 2% (w/v) dextrose), and non-fermentable YPEG medium (1% (w/v) yeast extract, 2% (w/v) bacto-peptone, 2% (w/v) ethanol, and 3% (w/v) glycerol), as indicated for each experiment. Solid medium contained 1.5% (w/v) agar. Cells were cultured at 30 °C unless specified otherwise.

Plasmid Construction—A single-copy yeast plasmid, p416-GPD (33), was used for *GPD1* gene promoter-mediated constitutive expression of *PCA1* and its mutant alleles. Triple hemagglutinin (3HA) and double c-myc (2Myc) epitopes were inserted after the start codon and before the stop codon of *PCA1*, respectively, for the detection of Pca1p expression. Fusion of these epitopes did not alter the function of Pca1p (30). *PCA1* mutant alleles were created with PCR-based site-directed mutagenesis using an overlapping primer method (34). The coding sequence of *SSA1* was PCR-amplified using a gene-specific primer set and inserted into the BamHI/XhoI sites of the p415-GPD plasmid (33). The HA epitope was fused at the C terminus. To purify the GST-fused *PCA1* fragment encompassing the amino acids 250–350 region (GST-Pca1p(250–350)) by *Escherichia coli* expression, the nucleotide sequence obtained by PCR using a gene-specific primer set flanked with the BamHI enzyme site and a stop codon followed by XhoI 5′ and 3′, respectively, was inserted into the pGEX-6P-1 vector (35).

The *YOR1* expression construct in p415-GPD was prepared by PCR amplification of the coding sequence of the *YOR1* gene in the BY4741 strain using a gene-specific primer set followed by ligation of it into the XbaI and XhoI sites of the vector. NotI site was artificially inserted right after the start codon. 3HA epitope-fused *PCA1(1–392)* was inserted into the NotI site. Site-directed mutagenesis was conducted by the primer overlap extension method (35) to create HindIII and PstI sites flanking *PCA1*(250–350) without altering amino acids.

Plasmid amplification and purification using *E. coli* followed molecular biology methods established previously (36). Yeast plasmid transformation was performed using a lithium acetate method (37).

Purification of Pca1p(250–350) Peptide—BL21 *E. coli* cells expressing the pGEX-6P-1 vector containing GST-Pca1(250–350)p or GST were grown to mid-log phase and induced with 50 μM isopropyl 1-thio-β-D-galactopyranoside overnight at 18 °C. Cells were collected and lysed by sonication in lysis buffer containing 50 mM Tris-HCl (pH 7.2), 100 mM sucrose, 10% (v/v) glycerol, 500 mM NaCl, 1 mM tris(2-carboxyethyl)phosphine (TCEP), 1 mM pepstatin A, and 1 mM PMSF. Lysates were then incubated with Triton X-100 (1%, v/v) at 4 °C for 30 min and centrifuged at 11,000 × *g* to remove cell debris. The resulting lysate was added to a glutathione-agarose column (Pierce) and incubated overnight with gentle rocking at 4 °C. The column was washed with wash buffer (20 mM Tris-HCl (pH 7.2), 100 mM sucrose 10% (v/v) glycerol, 150 mM NaCl, 1 mM TCEP, and 15 mM octyl-β-glucoside) and then treated with PreScission protease (100 units, GE Life Sciences) in the wash buffer. The purified Pca1p(250–350) was used for biophysical characterizations.

Metal-induced Tyrosine Quenching of Pca1p(250–350) Determined by Spectroscopy—Binding of Cd^{2+} to Pca1p(250–350) (in 50 mM Tris-HCl (pH 7.4) in the presence of 1 mM TCEP) through addition of increasing concentrations of $CdCl_2$ (0.625 μM) was determined by monitoring the quenching of tyrosine fluorescence. Excitation was set at 280 nm, and the emission was collected (38). Given the reducing environment in the cytosol, TCEP prevents oxidation of Cys residues. The same protocol was followed for copper and zinc; however, $CuCl_2$ solubilized in water was pretreated with ascorbate (1 mM) at 4 °C for 30 min to reduce Cu^{2+} to Cu^{+}. Cytosolic copper ions are in the Cu^{+} redox state; cadmium and zinc exist only in the divalent state.

Isothermal Titration Calorimetry—Purified Pca1p(250–350) (240 μM in 1.8-ml volume) was placed into the reaction chamber of a microcalorimeter (MicroCal VP-ITC), and 10 mM $CdCl_2$ was loaded into the syringe. The reaction was monitored for 18 injections with a total run time of 90 min, and the result-

ing data were plotted using MicroCal Origin software. This was repeated with $CdCl_2$ against the sample buffer to exclude $CdCl_2$ binding to the components (*e.g.* TCEP) of the reaction buffer.

Inductively Coupled Plasma MS—Cells were co-cultured with $CdCl_2$ (1 μM for 0–60 min) at the mid-log phase (A_{600} ~0.8). At each time point, cells were collected and washed once in medium (30 °C) containing EDTA (10 mM) to remove excess $CdCl_2$ bound to the cell surface. Cells (5 ml of A_{600} = 1 cell) were then thoroughly washed in ice-cold H_2O containing 10 mM EDTA and digested in 600 μl of 10% nitric acid at 70 °C for 2 h. Metal levels in the samples were measured by inductively coupled plasma MS as described previously (39). The cadmium concentration in cells at exponential growth phase was calculated using the average cell number of 3×10^7 cells/each A_{600} = 1 and an average cell volume of 42×10^{-15} 42 fl (40).

Generation of a PCA1(250–350) Random Mutant Library—*PCA1(250–350)* was PCR-amplified under an error-prone condition (41) using a primer set flanked with HindIII and PstI sites at the 5′ and 3′ ends, respectively. This library of *PCA1(250–350)* fragments contains a single amino acid change generated randomly per three fragments. PCR products replaced the corresponding fragment of a plasmid containing an N-terminal in-frame fusion of *PCA1(1–392)* with *YOR1*. Approximately 6000 *E. coli* colonies were obtained. The resulting colonies were pooled together and subjected to plasmid extraction.

Selection of Stabilized PCA1(1–392)-YOR1 Plasmids Containing Mutation(S) in PCA1(250–350)—PCA1(1–392)-YOR1 plasmids containing random mutation(s) in *PCA1(250–350)* were transformed to the *yor1*Δ yeast strain. Replicative plating of the colonies (~30,000) to plates containing oligomycin (1 μg/ml) selected yeast cells conferring Yor1p-dependent oligomycin resistance. Colonies growing on oligomycin plates were selected. The plasmid was extracted from the cells and amplified using *E. coli* (42). Sequencing of the plasmids identified mutation(s) within *PCA1(250–350)*.

Cell Growth Assay on Solid Medium Containing Oligomycin and/or Cadmium—Yeast cells expressing Pca1(1–392)-Yor1p, Yor1p, or Pca1p(1–392)-Yor1p possessing amino acid substitution(s) were cultured in SC-selective medium to mid-log phase. Cells (~5 μl, A_{600} 0.1) were spotted on solid YPEG medium prepared with and without the addition of cadmium ($CdCl_2$, 2 μM) or oligomycin (1 μg/ml). Plates were incubated at 30 °C for 2 days prior to photography (9).

Immunoblotting—Cells were broken using glass bead disruption in lysis buffer (PBS containing 0.1 mM PMSF, protease inhibitor mixture (Complete Mini, Roche), 0.1 mM EDTA, and 1% Triton X-100). The protein concentration of samples was measured using the BCA kit (Pierce) following the instructions of the manufacturer. Samples were denatured using sample buffer containing DTT (25 mM) and subjected to denaturation (37 °C for 15 min). SDS-PAGE was transferred to nitrocellulose membrane, and proteins were detected using rabbit anti-HA monoclonal antibodies (Rockland, 600-401-384), mouse anti-myc antibodies (ABM, G019), and mouse anti-3-phosphoglycerate kinase (Pgk1p) antibodies (Invitrogen, 459250). Horseradish peroxidase-conjugated goat anti-rabbit IgG (Santa Cruz Biotechnology Inc., SC-2005) and goat anti-mouse IgG (Santa Cruz Biotechnology Inc., SC-2004) were secondary antibodies. West Pico chemiluminescence (Thermo Scientific) was used for illumination of antibody-bound proteins.

Co-immunoprecipitation to Determine the Physical Interaction between Pca1p and Ssa1p—Pca1p fused with 3HA and 2Myc epitopes at the N and C termini, respectively, with and without L296S substitution and empty vector (p416-GPD) were co-expressed with Ssa1p-HA in *pdr5*Δ cells. Cells at mid-log phase (A_{600} ~0.8) were treated with a proteasome inhibitor (MG132, 20 μM) for 2 h. Cells were then collected by centrifugation (6000 × *g*, 5 min), washed in ice-cold PBS, and then resuspended in PBS containing MG132 (20 μM) and a membrane-permeable, thiol-reversible cross-linker, dimethyl 3,3′-dithiobispropionimidate (100 μg/ml) (Thermo Scientific). After incubation at room temperature with gentle rocking for 30 min, cells were placed on ice and washed in lysis buffer (50 mM Tris-HCl (pH 7.4), 0.1 mM EDTA, 0.1 mM PMSF, and protease inhibitor mixture (Complete Mini, Roche)) to quench the reaction. Cell lysates were obtained by glass bead disruption in the same buffer. Samples were spun down (300 × *g* for 3 min) to remove debris and unbroken cells. The lysates were then centrifuged (100,000 × *g* for 30 min) to create a pellet fraction. Pellets were treated with Triton X-100 (1%) for 30 min at 4 °C with gentle rocking for membrane solubilization. The protein concentration was measured using a BCA kit (Pierce). Cell lysates (1 mg) were incubated with anti-myc beads using a Profound™ c-Myc tag immunoprecipitation/co-immunoprecipitation kit (Thermo Scientific) according to the specifications of the manufacturer. Eluted proteins were treated with DTT (150 mM) to break the cross-links (37 °C for 30 min). The resulting solution was run on SDS-PAGE, followed by immunoblotting to detect the interaction between Pca1p and Ssa1p.

Alignment of Pca1p(250–350) with the Corresponding Sequence of Pca1p-like Proteins in Other Fungi—NCBI BLAST (43) identified closely related sequences to Pca1p(250–350). A ClustalW2-aligned (44) amino acid sequence was obtained from the search.

Prediction of Structure—I-TASSER predicted the three-dimensional structure of Pca1p(230–350) (45). The highest-scoring match was selected. Helical wheel projections of Pca1p(271–306) were obtained. Hydrophobic cluster analysis of Pca1p(250–350), and Pca1p(250–350) containing either the I299N or L296S substitution was conducted (46).

Statistical Analysis—Data were presented as mean ± S.D., and statistical comparisons of control and experimental groups were performed using Student's *t* test. $p < 0.05$ was considered to be significant.

Results

Determination of Cadmium Binding to Pca1p(250–350)—Pca1p in the yeast *S. cerevisiae* undergoes a rapid turnover by ERAD in a cadmium- and degron-dependent mechanism (9, 30). We aimed to gain a better understanding of how the ERAD machinery recognizes the degron in the absence of cadmium and how cadmium masks the signal. GST-fused Pca1p(250–350) peptide encompassing the 250th to 350th amino acids of Pca1p and containing the degron was expressed in *E. coli* and subsequently purified using GSH-agarose, followed by cleavage of the GST (Fig. 1*A*). The purified peptide was subjected to UV

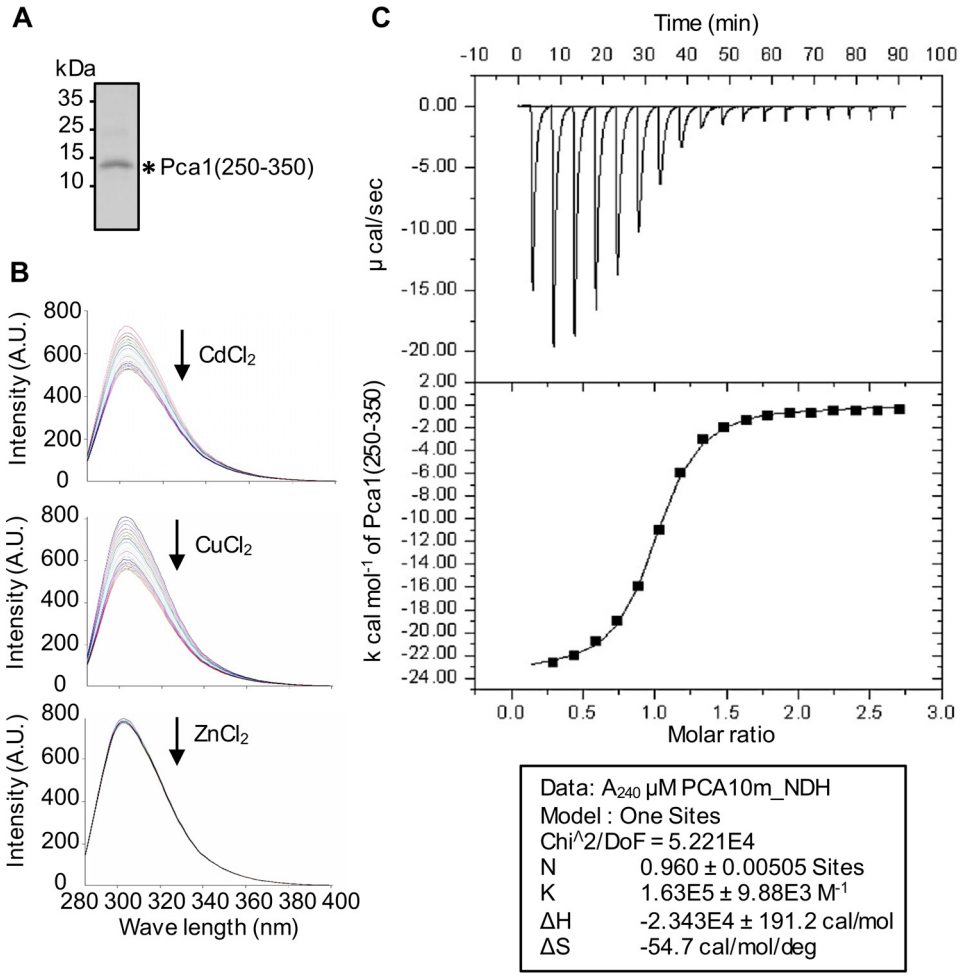

FIGURE 1. **Cadmium binding to Pca1p(250–350).** *A*, purification of Pca1p(250–350) peptide containing a cadmium-responsive degron. *B*, tyrosine quenching with the addition of metals using excitation/emission spectroscopy. Pca1p(250–350) (2 μM in 50 mM Tris-HCl (pH 7.4) in the presence of 1 mM TCEP) was mixed with $CdCl_2$, $CuCl_2$, and $ZnCl_2$ at concentrations from 0–6.25 μM in a cumulative manner, and emission intensity was monitored. *C*, binding of cadmium to Pca1p(250–350) determined by isothermal titration calorimetry. Pca1p(250–350) (5 μM in 50 mM Tris-HCl (pH 7.4) in the presence of 1 mM TCEP) was titrated with 5 μM $CdCl_2$ over 90 min. A representative figure of duplicated experiments is presented. *A.U.* indicates arbitrary unit.

fluorescence quenching after addition of cadmium, copper, or zinc spectroscopy. Although Pca1p(250–350) peptide does not contain any Trp residues, it does contain six Tyr residues. We were able to follow the change in emission spectra with the introduction of cadmium (Fig. 1*B*). Cadmium and copper but not zinc affected the emission spectra of the peptide; this is consistent with *in vivo* data displaying a metal ion specificity in inducing Pca1p stabilization in a manner dependent on the degron (9, 30). It is necessary to emphasize that the copper effect on Pca1p in cells was not observed in wild-type control strains that express the Ace1p-mediated copper detoxification system (30). Therefore, among tested metal ions, cadmium is the only regulator of the degron in Pca1p under physiologically relevant conditions. Isothermal titration calorimetry was utilized to determine the binding affinity of cadmium with Pca1p(250–350) (Fig. 1*C*). The disassociation constant (K_d = ~6 μM (1/*K*a, *K*a = 1.63×10^5 M^{-1})) was determined for this peptide when presented with $CdCl_2$ (Fig. 1*C*, *bottom panel*). The observed stoichiometric ratio of Cd^{2+} binding was one Cd^{2+} ion to one peptide (n = 0.96 or ~1).

Given the rescue of Pca1p from ERAD when cells are co-cultured with cadmium at 1 μM concentration, the K_d value was higher than anticipated. We addressed the possibility of intracellular cadmium accumulation over time to induce Pca1p stabilization. Indeed, the cadmium content of the cells co-cultured with 1 μM $CdCl_2$ reached 6.60 μM and 15.30 μM after 15 and 30 min, respectively (Fig. 2*A*). This surprisingly high accumulation of cadmium correlated well with Pca1p stabilization determined by Western blotting (Fig. 2*B*). Although it is necessary to note the differences between *in vivo* and *in vitro* environments affecting available cadmium to Pca1p(250–350), these data indicate that the 6.1 μM K_d for cadmium binding to the Pca1p(250–350) determined *in vitro* might be physiologically relevant.

Roles for Cysteine Residues of Pca1(250–350) in Cadmium Sensing—Cys residues are readily targeted by cadmium because of its high affinity for thiols (47). Pca1p(250–350) contains seven Cys residues, including those in the $CXCX^{10}CC$ motif (X = any amino acid) (Fig. 3*A*). To determine whether these residues are involved in cadmium sensing, the Cys residues were substituted with Ala (Fig. 3*B*). Cells expressing *PCA1* alleles possessing the mutations were cultured with and without cadmium (1 μM, 30 min), and steady-state Pca1p levels were measured by Western blotting (Fig. 3*B*). As expected, WT

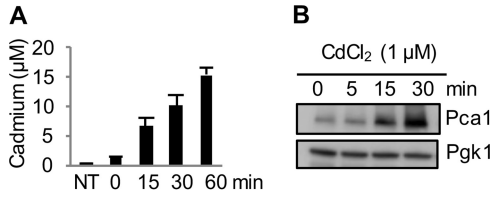

FIGURE 2. **Accumulation of cadmium in the yeast *S. cerevisiae* and Pca1p up-regulation.** *A*, the BY4741 yeast strain expressing non-functional *PCA1* because of natural mutation was co-cultured with $CdCl_2$ (1 μM in the medium) at mid-log phase and collected at the indicated time points. Total cell-associated cadmium was measured. The cadmium content in each cell was calculated based on cell numbers of the samples and the volume of each cell. The data indicate mean ± S.D. ($n = 9$). *B*, determination of Pca1p stabilization as an indicator of cellular cadmium accumulation. BY4741 cells expressing functional Pca1p fused with N-terminal 3HA by the constitutive *GPD1* gene promoter were cultured as described above. Western blotting of cell lysates using anti-HA antibodies visualized cadmium-induced expression of Pca1p. Pgk1p was detected with specific antibodies to determine equal loading. A representative figure of two independent experiments is presented. *NT* indicates a "no treatment" control.

Pca1p showed dramatic up-regulation when cells were co-cultured with cadmium (Fig. 3, *B*, *first lane versus second lane*, and *C*, *first column*). Substitution of either C*X*C or CC to Ala resulted in reduced cadmium effects on Pca1 stabilization (less than 50% relative to control Pca1p) (Fig. 3, *B*, *third lane versus fourth lane* and *fifth lane versus sixth lane*, respectively, and *C*, *second* and *third columns*). Other amino acid residues therefore could sense cadmium in the absence of two Cys residues at C*X*C or CC. However, when all seven Cys residues were substituted to Ala, there was a complete loss of cadmium-induced Pca1p stabilization (Fig. 3, *B*, *seventh lane versus eighth lane*, and *C*, *fourth column*). It is also intriguing to note the elevated steady-state expression levels of Pca1p possessing Ala substitution of CC or all seven Cys (Fig. 3, *B*, *first lane versus fifth* and *seventh lanes*, and *D*, *third* and *fourth columns*). This suggests inefficient recognition of those Pca1p by the ERAD machinery in the absence of cadmium exposure.

In an effort to determine whether the Cys residues work in concert to coordinate cadmium or whether it was simply due to the nonspecific thiol affinity of cadmium, Cys^{298} in the C*X*C and Cys^{311} in the CC motif were switched with Ser^{291} and Ser^{306}, respectively (Fig. 3*A*). This broke the C*X*C and CC motifs but maintained the same seven Cys residues in Pca1p(250–350). The lack of cadmium-induced stabilization of Pca1p(S291C,C298S,S306C,C311S) (Fig. 3*E*, *third* and *fourth lanes*) indicated the existence of a specific binding site for cadmium within Pca1p(250–350). Pca1p(S291C, C298S,S306C, C311S) is still a substrate of the ERAD system because its expression is high in a *doa10*Δ strain that lacks the E3 ligase essential for ERAD of Pca1p. This indicates that the Pca1p possessing four amino acid substitutions retains its dependence on the ERAD system for degradation but cannot sense cadmium (Fig. 3*E*, *fifth* and *sixth lanes*). Collectively, these results suggest that the distribution of Cys residues is critical for cadmium sensing but not composition of a protein degradation signal.

Identification of Residues in Pca1p(250–350) Composing a Degron—The identity and characteristics of most degrons are poorly defined despite regulated turnover of a number of proteins. Our data indicate that, although the Cys residues in Pca1p(250–350) play a role in cadmium sensing to mask a degron, these residues are not critical for recognition of Pca1p by the ERAD system in the absence of cadmium. We therefore sought to identify amino acid residues comprising the degron in Pca1p(250–350).

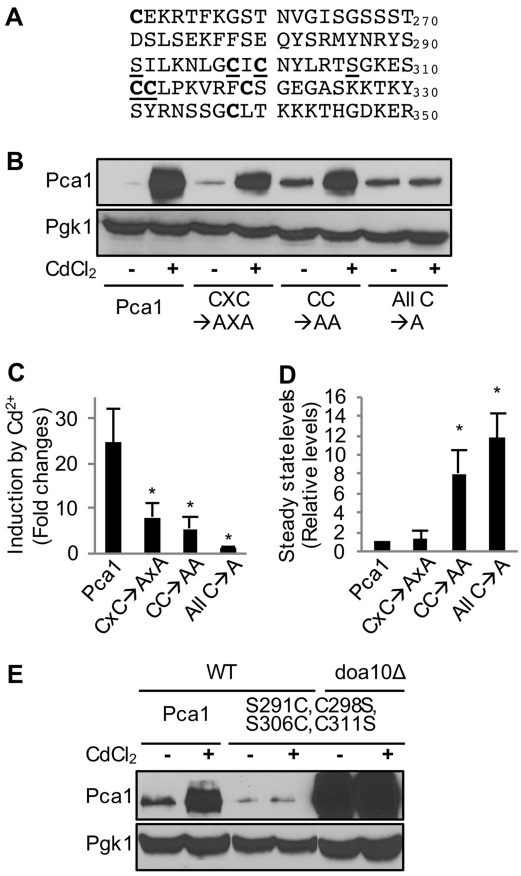

FIGURE 3. **Roles for cysteine residues of Pca1p(250–350) in cadmium-induced Pca1p stabilization.** *A*, amino acid sequence of Pca1p(251–350) with cysteine residues shown in *bold*. C*X*C and CC are *underlined*. Serine residues that exchange their positions with the first Cys residues of C*X*C and CC are *underlined*. *B*, the *GPD1* gene promoter-mediated expression constructs of functional Pca1p with and without site-directed mutation of Cys residues in *PCA1(250–350)* were transformed to a pca1Δ strain. *PCA1* was fused with N-terminal 3HA. Cells co-cultured with $CdCl_2$ (1 μM for 30 min) at mid-log phase were subjected to total cell lysate preparation. Western blotting with anti-HA antibodies determined expression levels of Pca1p. Pgk1p levels were used to determine equal loading. A representative figure of four repeats is presented. *C* and *D*, quantification of the data presented in *B*. Cadmium-induced changes in expression levels of the indicated Pca1p were measured (*C*). Steady state levels of Pca1p in cells cultured without cadmium were presented as relative levels of control Pca1p (*D*). *, $p < 0.01$ compared with wild-type control Pca1p. *E*, expression levels of Pca1p possessing S291C, C298S, S306C, and C311S substitutions were determined in WT control and *doa10*Δ cells as described in *B*. Representative data of two independent experiments are presented.

To be defined as a degron, the fusion of Pca1p(1–392) containing a degron with other proteins should result in regulation of their expression in a degron-dependent manner. Yor1p in yeast is a multidrug resistance protein extruding oligomycin, a mitochondrial toxin (48). Given the rapid turnover of Yor1p when it is fused with Pca1p(1–392), expression of Pca1p(1–392) did not confer oligomycin resistance (Fig. 4*A*). However, cadmium co-culture stabilized Pca1p(1–392)-Yor1p to allow cell growth at a lethal concentration of oligomycin (Fig. 4, *A* and *B*).

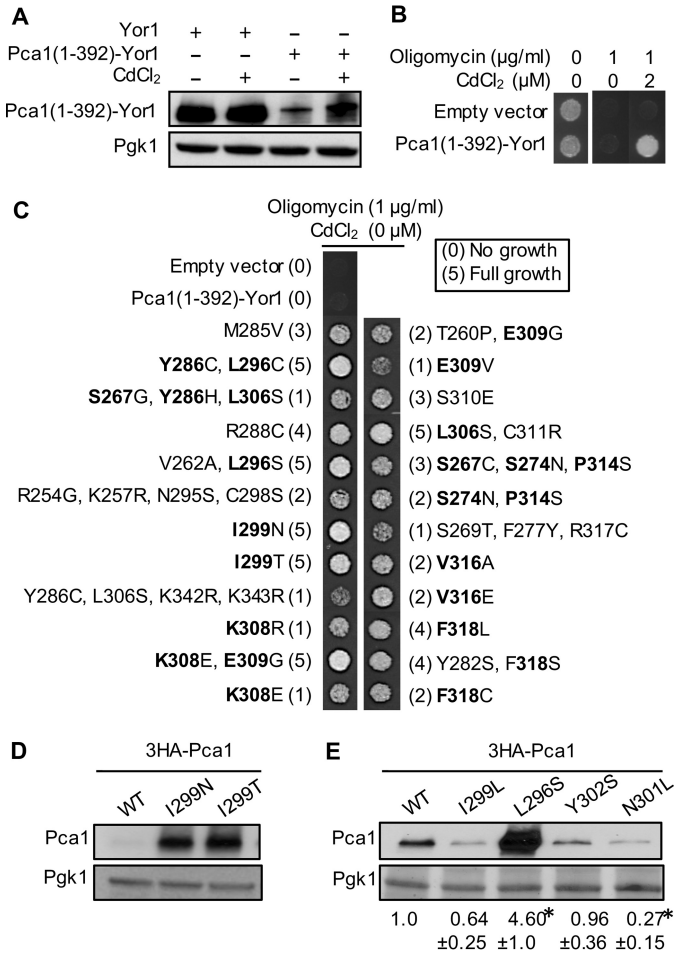

FIGURE 4. **Identification of residues required for the functional role of Pca1p(250–350) as a degron.** *A*, a *GPD1* gene promoter-mediated expression construct of Yor1p with and without fusion of Pca1p(1–392) at the N terminus (Pca1(1–392)-Yor1) was transformed into BY4741 yeast cells. GFP was fused in-frame at the N terminus. Western blots using anti-GFP antibodies determined expression levels of Pca1p(1–392)-Yor1p in cells with and without cadmium ($CuCl_2$) co-culture. *B*, growth of cells expressing empty vector and Pca1p(1–392)-Yor1p was examined on SC medium with and without supplementation of oligomycin and $CdCl_2$ at the indicated concentrations. Cells at mid-log phase were spotted on solid medium, and cell growth was photographed in 2 days. *C*, *PCA1(250–350)* fragments containing random mutation(s) generated by error-prone PCR and flanked with HindIII and PstI sites were replaced with the corresponding fragment in *PCA1(1–392)-YOR1*. The plasmid library was transformed into yeast cells to select cells that can grow on solid medium containing a lethal concentration of oligomycin. Plasmids were retrieved from growing cells and subjected to sequencing. The growth of BY4741 yeast cells expressing empty vector, wild-type control Pca1p(1–392)-Yor1p, or selected plasmids containing amino acid substitution(s) within Pca1p(250–350) was examined on solid SC medium containing oligomycin (1 μg/ml). Cell growth was photographed in 3 days. The relative oligomycin resistance of cells was rated using cells expressing Pca1p(1–392)-Yor1p containing Pca1p(I299N) substitution as the highest (5, full growth) and wild-type control Pca1p(1–392)-Yor1p as the lowest (0, no growth). Several plasmids contained more than one mutation. The quantitation was confirmed by at least two independent experiments. *D* and *E*, Western blot using anti-HA antibodies determined steady-state expression levels of Pca1p with and without the indicated site-directed mutations. 3HA was fused at the N terminus (*3HA-Pca1p*). The *GPD1* gene promoter-mediated expression constructs of 3HA-Pca1p were transformed into a *pca1*Δ strain. Cell lysates were subjected to Western blotting using anti-HA and -Pgk1p antibodies. A representative figure of four experiments is presented. *E*, the results of four experiments are quantitated and presented as -fold change in expression levels. *, $p < 0.01$.

We employed this experimental system to identify residues in Pca1p(250–350) that are recognized by the ERAD machinery. We hypothesized that substitution(s) of the amino acid residue(s) within Pca1p(250–350) that determine degron characteristics would stabilize Pca1p(1–392)-Yor1p, followed by oligomycin resistance without the introduction of cadmium. A library of Pca1p(250–350) fragments possessing random mutation(s) was generated by an error-prone PCR method (41). The pool of Pca1p(250–350) fragments flanked with restriction enzyme sites was ligated with the corresponding enzyme sites artificially created at the same location in Pca1p(1–392)-Yor1p. The Pca1p(1–392)-Yor1p expression library containing random mutation(s) at the region of Pca1p(250–350) was transformed in yeast cells, and then the cells were selected on solid medium containing oligomycin at a concentration displaying no growth of cells that express wild-type Pca1p(1–392)-Yor1p (Fig. 4*B*). Pca1p(1–392)-Yor1p expression plasmids were retrieved from growing colonies. Sequencing of the Pca1p(250–350) region of the plasmids identified mutations. Retransformation of each plasmid to yeast cells followed by oligomycin resistance confirmed the functionality of Pca1p(1–392)-Yor1p possessing specific mutation(s) (Fig. 4*C*). Each mutation conferred oligomycin resistance at different degrees. The vast majority of these mutations occurred in the region between amino acids 271–320, indicating the importance of the region in regulation of Pca1p. Interestingly, those conferring the strongest growth of cells (*e.g.* I299N, I299T, and L296S) contain a hydrophobic-to-hydrophilic substitution (Fig. 4*C*). When the mutations were introduced to the full-length *PCA1*, these mutations also resulted in cadmium-independent stabilization of Pca1p (Fig. 4*D*). To determine the specificity and underlying mechanisms, we also generated *PCA1* alleles by site-directed mutagenesis, including I299L (hydrophobic to hydrophobic), Y302S (hydrophilic to hydrophilic), and N301L (hydrophilic to hydrophobic). These *PCA1* alleles did not lead to Pca1p stabilization, which is distinct from L296S (hydrophobic to hydrophilic) (Fig. 4*E*). Moreover, it is interesting to note the reduced steady-state levels of Pca1p(N301L) (Fig. 4*E*, *fifth lane*) with the addition of a hydrophobic amino acid. These results collectively suggest that the composition of amino acid residues, especially hydrophobic residues within the amino acid 271–320 region, is critical for the functionality of the degron.

Although mutations were introduced randomly throughout *PCA1(250–350)*, most mutations, except a few that were identified in combination with other mutation(s), were located in the Pca1p(271–320) (Fig. 4*C*) region, suggesting that the region contains major characteristic(s) for the degron. Database searches for proteins containing homologous sequences of Pca1p(271–320) identified only Pca1p-like proteins in other fungi (Fig. 5). The corresponding sequence of Pca1p(271–320) in the identified proteins displayed several conserved amino acids (Fig. 5), including C*X*C and CC, which are important for cadmium sensing, and Leu^{296}, Ile^{299}, and Glu^{309}, which are critical for the functionality of the degron (Fig. 4*C*). This indicates that Pca1p in other fungi might be regulated by cadmium in a similar manner as in *S. cerevisiae*; however, the primary amino acid sequence of Pca1p(271–320) is not sufficient to identify degrons in unrelated proteins.

Characteristics of a Degron in Pca1p(250–350)—Given the lack of sequence similarity of Pca1p(250–350) with any structurally characterized protein, we predicted its secondary struc-

```
S.c.  271 DSLSEK-FFSEQYSRMYNRYSSILKNLGCICNYLRTLGKESCCLPKVRFCS 320
A.f.  122 GATDHK-ACSQHSLSALDRYGATLQALGCICRALIALGQETCCEIRERRSL 171
G.z.   23 GATDGK-PCNKHIVSALDRYGATLQALGCLCRTLISMGQESCCETRDRPA- 71
P.j.    1 ----HK-ACSQHSLSALDRYGATLQALGCICRALIALGQETCCEIRERQTL 46
A.c.  122 GATDRK-ACSQHNLSALDRYGATLQALGCICRALIALGQETCCEIRGRQAL 171
B.f.   71 LPSDEE-PCQSHLSKAKAAYSEILNNFGCICKVLLSLNLESCCALESGTVR 120
S.s.  130 -TKNKKGPCQSHMQSAKSRFQPTLDALECICRTLFALNLESCCSKIDNTSC 179
                :   ..:       :   *. : *:*. * ::. *:**
```

FIGURE 5. **Alignment of the Pca1p(271–320) sequence with the corresponding sequence of Pca1p-like proteins.** *Aspergillus fumigatus* (*A.f.*), *Gibberella zeae* (*G.z.*), *Penicillium janthinellum* (*P.j.*), *Aspergillus clavatus* (*A.c.*), *Botryotinia fuckeliana* (*B.f.*), and *Sclerotinia sclerotiorum* (*S.s.*) possess Pca1p-like proteins that correspond to GenBank numbers 3510005, 2791550, 156536662, 4708560, 5432339, and 5485834, respectively. The amino acid sequence of Pca1p(271–320) was aligned with the corresponding sequence of those in the identified proteins. *Asterisks* indicate that all sequences aligned contain the same residue at that location. The conserved residues, including four Cys, are also highlighted in *bold*. A *double dot* (:) indicates conservation among the displayed sequences with a single exception. A *single dot* (.) represents a low level of conservation of amino acid type.

ture using the I-TASSER program (45). A long helix encompassing Pca1p(271–306) followed by an unstructured loop and two short β sheets was observed (Fig. 6*A*). The C*X*C and CC motifs are localized near the end of the helix and in the middle of loop, respectively. Another Cys residue is located at the first β sheet (Fig. 6, *A* and *C*). This helix is amphipathic (Fig. 6*B*). All single mutations negating the degron were distributed within Pca1p(271–320) corresponding to the helix, loop, and first β sheet (Fig. 6*C*). The hydrophobic residues in the helix form a patch (Fig. 6*E*), which is consistent with the amphipathic nature of the helix (Fig. 6*B*). Three mutations, including I299T, I299N, and L296S, which lead to a non-functional degron and dramatic increase in Pca1p stabilization (Fig. 4, *C* and *D*), perturb the helix and hydrophobic cluster (Fig. 6, *D* and *F*). Collectively, these data suggest that amino acid distribution forming an amphipathic helix and hydrophobic patch is a critical characteristic of the degron.

Physical Interaction between Pca1p(250–350) and Ssa1p in a Manner Dependent on Cadmium and Amino Acid Residues—Surface exposure of hydrophobic residues in unfolded, misfolded, or denatured proteins is considered a primary determinant of recruiting molecular chaperones. It has been proposed that ERAD substrates are recognized by molecular chaperones, especially Hsp70s, to be targeted to the ubiquitination machinery (18, 49). The hydrophobic patch in the helix of Pca1p(250–350) (Fig. 6, *B* and *E*) is within the predicted cytosolic domain (31). Therefore, the degron might attract molecular chaperones, but cadmium sensing could induce a conformational change to hide the signal. We tested this hypothesis by determining a physical interaction between Ssa1p, an Hsp70p, and Pca1p in the cells expressing WT control Pca1p without or with cadmium co-culture (Fig. 7*A*, *third* and *fourth lanes*, respectively) or Pca1p possessing the L296S substitution (Fig. 7*A*, *fourth lane*), which leads to stabilization of Pca1p without cadmium co-culture. Cells co-expressing Pca1p tagged with double c-myc epitopes (Pca1p-2myc) and Ssa1p tagged with a triple HA epitope (Ssa1p-HA) using the constitutive *GPD1* gene promoter were cultured with and without cadmium in the medium (1 μM, 1 h). After treating cells with dimethyl 3,3′-dithiobispropionimidate, a cell-permeable cross-linker, membrane fractions were obtained. Pca1p-2Myc was immunoprecipitated using anti-myc antibodies and probed with anti-myc antibodies and anti-HA antibodies to detect Pca1p and Ssa1p, respectively (Fig. 7*A*). Although immunoprecipitated Pca1p is ~9-fold higher in cells co-cultured with cadmium, Ssa1p association with Pca1p was less than 15% (13.4 $\pm$ 1.5%, $n = 2$) that of control cells (Fig. 7*A*, *third* and *fourth lanes versus second lane* in the *first* and *second panels*). This result suggests that cadmium sensing by Pca1p interferes with its binding to Ssa1p, presumably by masking the hydrophobic patch within Pca1p(271–320). To address this, we compared the complex formation of Ssa1p with control Pca1p and Pca1p(L296S). The L296S substitution perturbed the hydrophobic patch in the Pca1p(271–320) region and resulted in Pca1p stabilization (Figs. 6*F* and 7*A*, *fourth lane*). Indeed, the pulldown efficiency of Ssa1p by Pca1p(L296S) was less than 20% (15.7 $\pm$ 5, $n = 2$) of control Pca1p (Fig. 7*A*, *fourth lane*). Western blotting displayed that Pca1p levels in *ssa1*Δ cells are higher, which is further increased by cadmium co-culture (Fig. 7*B*). Given no significant change in the expression levels of Pca1p in cells lacking all three other Ssa1p isoforms (*ssa2,3,4*Δ), Ssa1p plays a major role in the steady-state expression of Pca1p (Fig. 7*C*). This argument was confirmed using an *ssa2,3,4*Δ strain expressing an *Ssa1–45* allele. In the strain, Pca1p expression levels were significantly higher relative to those of WT and *ssa2,3,4*Δ strains expressing the functional Ssa1p (Fig. 7*C*). Although *Ssa1–45* was isolated as a temperature-sensitive allele (32), no obvious difference in Pca1p expression was observed between the permissive and restrictive temperatures. To determine the physiological significance of Pca1p stabilization in the absence of Ssa1p, cells expressing Ssa1p or Ssa1–45p were co-cultured with cadmium (1 μM $CdCl_2$, 30 °C, 30 min), and then cellular cadmium levels were measured (Fig. 7*D*). As anticipated, Pca1p expression decreased cellular cadmium levels. The strain expressing high levels of Pca1p because of the partially functional Ssa1–45p accumulated significantly less cadmium relative to strains expressing fully functional Ssa1p (Fig. 7*D*). These results collectively suggest that hydrophobic amino acid residues within the degron (*e.g.* L296) recruit Ssa1p to induce ERAD of Pca1p. However, cadmium sensing interferes with the interaction to induce Pca1p expression, followed by cadmium detoxification.

Discussion

Despite many examples of regulated turnover of proteins, the identity, characteristics, and control mechanisms of degradation signals have been defined for only a few proteins. The results presented in this manuscript reflect one of best-characterized degrons.

Purified Pca1p(250–350) containing a degron displayed binding with cadmium and copper but not zinc, which is con-

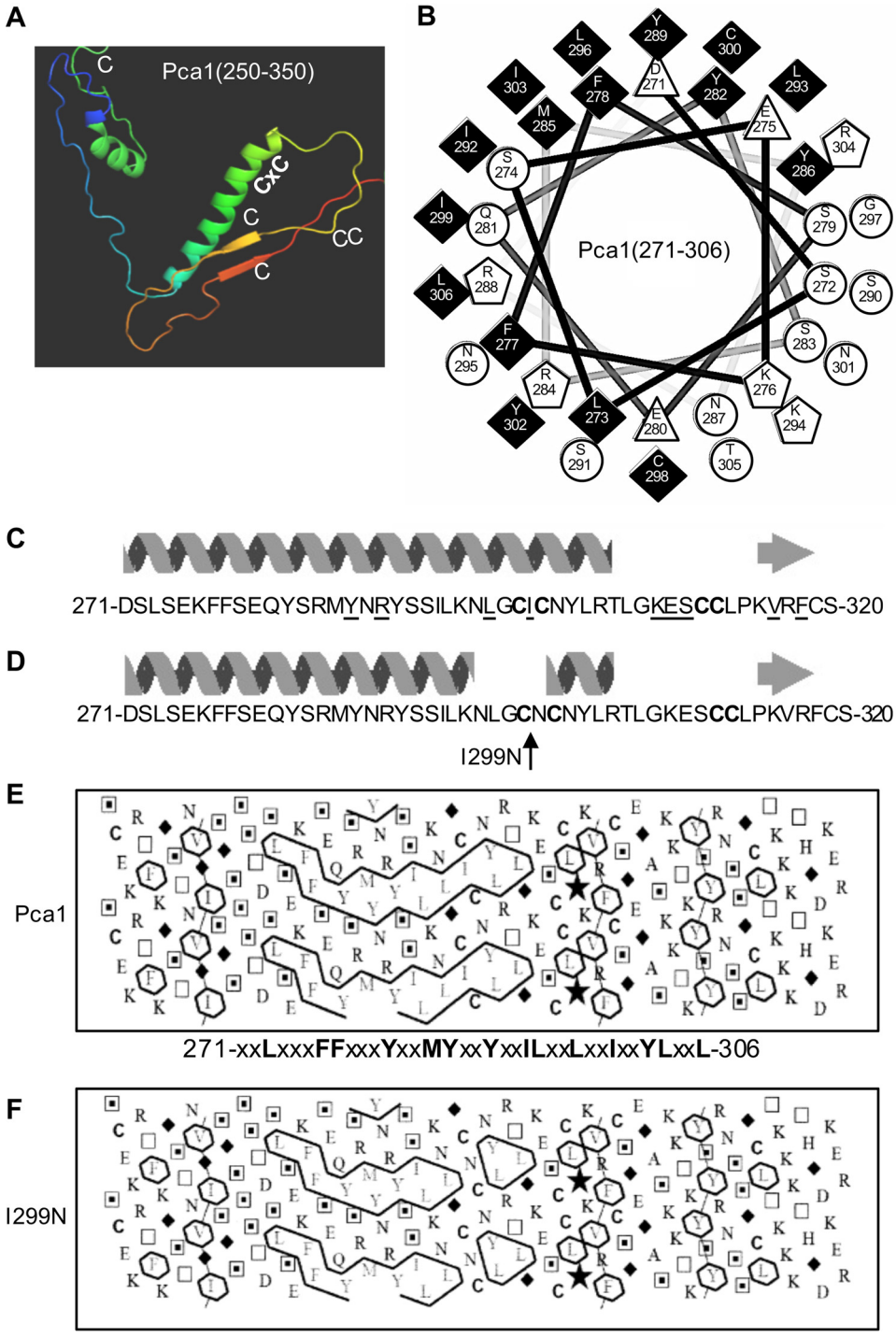

FIGURE 6. **Prediction of the secondary structure of Pca1p(250–350) and amino acid substitution affecting Pca1p expression.** *A*, the predicted structure of Pca1p(250–350). Seven Cys residues are indicated. *B*, distribution of amino acids within the Pca1p(271–306) helix predicted by helical wheel projection analysis. *Filled diamonds*, *circles*, *triangles*, and *pentagons* indicate hydrophobic, hydrophilic, potentially negative charged, and potentially positively charged residues, respectively. *C*, predicted secondary structure of Pca1p(271–320). The *underlined* residues indicate confirmed substitutions that affect Yor1p stabilization and Yor1p-mediated oligomycin resistance when Pca1p(1–350) containing the individually substitution is fused with Yor1p. *D*, perturbation of the secondary structure of Pca1p(271–320) by I299N substitution. *E*, formation of a hydrophobic patch by amino acids within Pca1p(271–306) obtained by hydrophobic cluster analysis. Amino acids that are involved in the formation of the hydrophobic patch are indicated by the *outline*. The amino acids are presented by their one-letter identification, except for glycine residues, which are represented by *black diamonds*, serines, which are *black squares with a dot in the middle*, and threonines, which are represented by *black open squares*. *F*, disruption of a hydrophobic patch within Pca1p(271–320) by I299N substitution.

sistent with metal specificity in the stabilization of Pca1p in yeast cells (30, 31). Nevertheless, it is important to note that Pca1p stabilization by copper was only evident in a strain deficient of the Ace1p transcription regulator, which induces expression of copper-chelating metallothionein (MT), but not wild-type control cells (31). This result indicates that the copper binding sensitivity to Pca1p(250–350) is lower than Ace1p and MT. It was reported that cadmium binds to MT but does

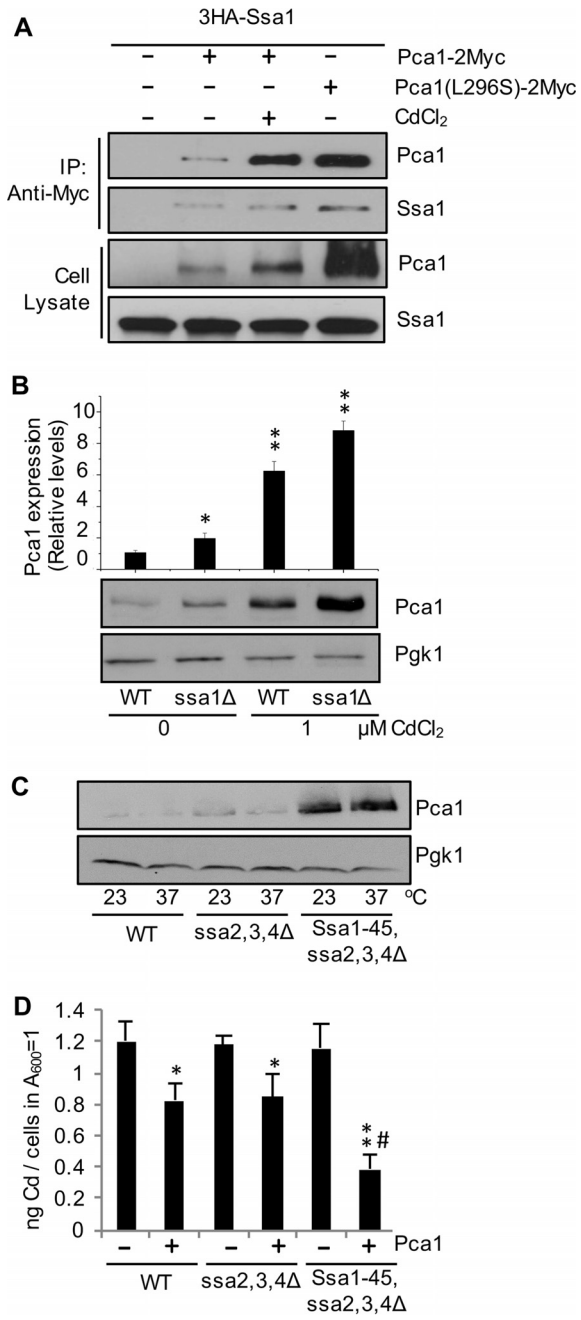

FIGURE 7. **Physical interaction between Pca1(250–350)p and a Hsp70p in a cadmium- and amino acid composition-dependent manner.** *A*, yeast cells expressing Pca1p tagged with two c-myc epitopes (*Pca1p-2Myc*) and Ssa1p tagged with a triple HA epitope (*3HA-Ssa1p*) were co-cultured with and without $CdCl_2$ (1 μM) for 1 h, and Pca1p(L296S)-2Myc (no $CdCl_2$) was treated with the membrane-permeable cross-linker dimethyl 3,3′-dithiobispropionimidate (100 μg/ml). Cell lysates were subjected to Western blotting using anti-HA and anti-myc antibodies. Pgk1p was detected using specific antibodies to determine equal loading. Immunoprecipitation (*IP*) of Pca1p-2Myc in the lysates was carried out using anti-myc-conjugated beads (Pierce). Pca1p-2Myc and 3HA-Ssa1p in the eluted samples were detected by Western blotting. *B*, Western blotting analysis of Pca1p in WT and *ssa1*Δ cells with and without cadmium co-culture (1 μM $CdCl_2$, 1 h). *, $p < 0.05$; **, $p < 0.01$; relative to WT control (*first lane*). *C*, Western blot of Pca1p expressed in the indicated yeast strains that were cultured at permissive (23 °C) and restrictive (37 °C) temperatures for 2 h. *D*, the indicated strains carrying an empty vector or Pca1p expression plasmid were co-cultured with cadmium (1 μM $CdCl_2$, 30 min). Cellular cadmium levels were measured. *, $p < 0.05$; **, $p < 0.01$; relative to a corresponding strain containing an empty vector (−*Pca1*). #, $p < 0.01$ relative to the WT and *ssa2,3,4*Δ strain expressing Pca1p. A representative figure and/or mean ± S.D. of two (*A*) or three (*B*, *C*, and *D*) experiments are presented.

not activate Ace1p to increase expression of MT (50). Consistently, cadmium-induced stabilization of Pca1p was observed in WT cells (31). The selectivity of Pca1p(250–350) to cadmium *versus* zinc remains to be investigated because of the similar characteristics between the elements and documented examples of sharing binding sites and transporters (47, 51, 52).

The half-life of proteins is determined by various mechanisms such as intrinsic signatures (*e.g.* N-terminal amino acid, PEST sequences), cellular regulation (*e.g.* posttranslational modification of proteins recruiting degradation machinery), and folding failure and damage (1, 53, 54). It was shown that cell-permeable agonists and antagonists elevated the expression of wild-type control and mutated δ opioid receptors that are degraded by ERAD (55). Binding of estrogen to the estrogen receptor α controls the pathways of estrogen receptor α degradation (56). Turnover of apolipoprotein B and Hmg2p in response to limitation of lipid molecules and surplus of intermediates of sterol biosynthesis, respectively, are other examples of ligand-dependent protein turnover (13, 57). However, Pca1p is unique in that cadmium directly binds to a degron in Pca1p to control its accessibility. It is interesting to speculate that small molecules, such as inorganic species, xenobiotics, substrates, ligands, and metabolites, might be widely involved in the regulation of protein turnover.

Given the critical role of Pca1p(250–350) as a sensor of cadmium to stabilize Pca1p, the relatively high K_d (~6 μM) of Pca1p(250–350) for cadmium was an unanticipated outcome. For instance, it was shown that the CueR transcription activator of copper efflux genes in *E. coli* manifests zeptomolar sensitivity to free Cu^+ (58). Nevertheless, cells co-cultured with 1 μM $CdCl_2$ accumulate ~6 μM cadmium within 15 min, which was correlated with Pca1p stabilization. Nevertheless, it is necessary to point out that the cadmium concentration does not reflect cadmium ions in the fluid phase of the cytoplasm. Given no available method for measuring the labile pool of cadmium in the cytoplasm, the cadmium sensitivity of the degron in cells warrants further research.

It is worth considering the possibility that cadmium sensing by Pca1p(250–350) is promoted by specific factor(s) that could increase the efficiency of cadmium sensing. GSH, an abundant (low micromolar concentration) tripeptide transfers cadmium to the Ycf1p cadmium transporter in the vacuolar membrane (59). Our study however indicated that the cadmium binding of Pca1p(250–350) *in vitro* is not affected by reduced and oxidized GSH and cysteine in the reaction buffer (data not shown). This suggests that the cadmium binding affinity is higher for Pca1p(250–350) relative to that for GSH and free cysteine. It was reported that the Atx1p metallochaperone can bind both cadmium and copper (60). However, our previous data showed that Pca1p function is not affected in the absence of known copper chaperones (41). Cadmium chaperone(s) for the degron in Pca1p, if they exist, remain to be identified.

Pca1p(250–350) contains seven Cys residues that are frequently identified at metal binding sites in other proteins (61). Metal-sensing transcription regulators such as Mac1p and Ace1p in yeast and MTF-1 in higher eukaryotes, including mammals, also rely on Cys residues that likely bind with metal ions as a sensing mechanism (62). Other common amino acid

residues involved in metal sensing are histidine and methionine. Endocytosis and degradation of a human zinc importer in a histidine-rich, cluster-dependent manner protects against zinc cytotoxicity (63). Several other P_{1B}-type ATPase family members in mammals and plants to which Pca1p belongs possess undercharacterized metal-binding residues at the N or C terminus (64). The predicted metal binding sites might play roles for regulation of activities, expression, and/or subcellular trafficking of those transporters.

Only Pca1p-like proteins in other fungi contain a similar amino acid sequence to Pca1p(271–320), the core sequence composing a degron in Pca1p. This indicates that the primary sequence of the degron in Pca1p does not provide useful information for identifying degrons in other unrelated proteins. Our attempts for obtaining secondary and tertiary structures of Pca1p(250–350) with and without cadmium sensing have not been successful, which is primarily attributed to aggregation of purified Pca1p(250–350) at the concentrations required in solution experiments and crystallization. Nevertheless, identification of amino acid residues within Pca1p(271–350) that are responsible for its function as a degron reveals a critical role of the residues forming a hydrophobic patch on a predicted amphipathic helix of Pca1p(271–306). The exposure of hydrophobic residues at the surface of proteins resulting from misfolding or denaturation has been considered as the signal for recruiting molecular factors involved in refolding and destruction (16). Given Pca1p stabilization by site-directed substitution of several amino acids in the predicted loop and β sheet that follows, those mutations could mimic cadmium sensing and perturb the degradation signal.

The degradation signals of two known ERAD substrates, Matα2p of yeast and mammalian SGK1, have been characterized as amphipathic helices (16, 17). Intermolecular interaction masks the signal in Matα2p (16); however, it is uncertain whether the degron in SGK1 is regulated by cellular cues as a mechanism of expression control. A non-biased selection of 16–50 amino acid peptides revealed that hydrophobic amino acid clusters can serve as signals for degradation (65). Determination of the contribution of each amino acid in one of the peptides by site-directed mutagenesis confirmed that both a patch of bulky hydrophobic residues and positively charged residues were found to be essential, which is distinct from the degrons in Matα2p and SGK1 (66). These reports are in line with our results indicating the roles for hydrophobic residues and two positively charged residues, Arg^{288} and Lys^{308} (Fig. 6*C*). We also identified a negatively charged residue, Glu^{309} (Fig. 6*C*), which is unique for Pca1p. However, all of these characterized signals do not display any sequence homology to each other. Therefore, it is evident that the primary amino acid sequence is insufficient to predict degrons. Integration of secondary and tertiary structures of a particular protein and its interactions with other proteins and small molecules may achieve this. With continuous efforts to identify such signals from different targets, one could develop algorithms by which the signal(s) in each protein could be predicted and provide methods for controlling the signals via physiological or pharmacological means. This is an important issue because various diseases are implicated in an imbalance in protein expression and turnover (5, 67, 68).

It has been suggested that molecular chaperones are primarily responsible for recognition of the substrates of ERAD (69). Our data displayed that Ssa1p, an Hsp70p chaperone, physically interacts with Pca1p. The reduced interaction displayed by less efficient immunoprecipitation of Ssa1p with Pca1p is correlated with stabilization of Pca1p. Given that surface exposure of hydrophobic residues can serve as a signal for recruiting molecular chaperones, our result supports the notion that the patch of hydrophobic amino acids at the helix Pca1p(271–306) is recognized by Ssa1p. Cadmium binding to the degron limits its interaction with Ssa1p, indicating that cadmium serves as a natural chemical chaperone masking the degron. Molecular chaperones were initially characterized as heat stress-induced proteins that play critical roles in protein folding. Surface exposure of hydrophobic residues in a degron of Pca1p and misfolded or denatured proteins could be a common feature attracting molecular chaperones. However, it is still unclear exactly what determines the fate, folding *versus* degradation, of heat stress-induced protein clients.

Identification of small molecules that can improve the maturation and secretion of CFTRΔF508, which is associated with cystic fibrosis, the most common lethal genetic disease in Caucasians, has been actively explored (70). Co-culture of cells expressing CFTRΔF508 with glycerol restored its chloride transport function (71) The effects of glycerol were also observed for a mutated hERG potassium channel (72) and yeast Hmg2p (73). This has also been proposed as a treatment in neurodegenerative diseases manifesting an accumulation of misfolded proteins, such as Alzheimer, Parkinson, Huntington, and prion diseases (74). Cadmium and copper as a folding factor for the degron in Pca1p provides a new conceptual frame for further determination of chemical chaperone roles for ions and metabolites.

Author Contributions—N. S., W. W., and J. L. designed the research and analyzed the data. N. S., W. W., M. Z., X. Q., J. S., and H. K. performed the experiments. N. S., W. W., and J. L. wrote the manuscript. All authors reviewed the results and approved the final version of the manuscript.

Acknowledgments—We thank Dr. Ben Arentson (University of Nebraska, Lincoln) for technical assistance and helpful discussions and Dr. E. Craig (University of Wisconsin, Madison) for the ssa2,3,4Δ, ssa1–45,ssa2,3,4Δ, and isogenic control yeast strains.

References

1. Ravid, T., and Hochstrasser, M. (2008) Diversity of degradation signals in the ubiquitin-proteasome system. *Nat. Rev. Mol. Cell Biol.* **9,** 679–690
2. Hochstrasser, M. (1996) Protein degradation or regulation: Ub the judge. *Cell* **84,** 813–815
3. Zhang, K., and Kaufman, R. J. (2004) Signaling the unfolded protein response from the endoplasmic reticulum. *J. Biol. Chem.* **279,** 25935–25938
4. Babst, M. (2014) Quality control: quality control at the plasma membrane: one mechanism does not fit all. *J. Cell Biol.* **205,** 11–20
5. Ansari, N., and Khodagholi, F. (2013) Molecular mechanism aspect of ER stress in Alzheimer's disease: current approaches and future strategies. *Curr. Drug Targets* **14,** 114–122

6. Bukau, B., Weissman, J., and Horwich, A. (2006) Molecular chaperones and protein quality control. *Cell* **125,** 443–451
7. Mollereau, B., Manié, S., and Napoletano, F. (2014) Getting the better of ER stress. *J. Cell. Commun. Signal.* **8,** 311–321
8. Schrader, E. K., Harstad, K. G., and Matouschek, A. (2009) Targeting proteins for degradation. *Nat. Chem. Biol.* **5,** 815–822
9. Adle, D. J., Wei, W., Smith, N., Bies, J. J., and Lee, J. (2009) Cadmium-mediated rescue from ER-associated degradation induces expression of its exporter. *Proc. Natl. Acad. Sci. U.S.A.* **106,** 10189–10194
10. Kanarek, N., London, N., Schueler-Furman, O., and Ben-Neriah, Y. (2010) Ubiquitination and degradation of the inhibitors of NF-κB. *Cold Spring Harb. Perspect. Biol.* **2,** a000166
11. Alkalay, I., Yaron, A., Hatzubai, A., Orian, A., Ciechanover, A., and Ben-Neriah, Y. (1995) Stimulation-dependent I κ B α phosphorylation marks the NF-κ B inhibitor for degradation via the ubiquitin-proteasome pathway. *Proc. Natl. Acad. Sci. U.S.A.* **92,** 10599–10603
12. Fukutomi, T., Takagi, K., Mizushima, T., Ohuchi, N., and Yamamoto, M. (2014) Kinetic, thermodynamic, and structural characterizations of the association between Nrf2-DLGex degron and Keap1. *Mol. Cell. Biol.* **34,** 832–846
13. Fisher, E. A., and Ginsberg, H. N. (2002) Complexity in the secretory pathway: the assembly and secretion of apolipoprotein B-containing lipoproteins. *J. Biol. Chem.* **277,** 17377–17380
14. Bruick, R. K., and McKnight, S. L. (2001) A conserved family of prolyl-4-hydroxylases that modify HIF. *Science* **294,** 1337–1340
15. Varshavsky, A. (1991) Naming a targeting signal. *Cell* **64,** 13–15
16. Johnson, P. R., Swanson, R., Rakhilina, L., and Hochstrasser, M. (1998) Degradation signal masking by heterodimerization of MATα2 and MATa1 blocks their mutual destruction by the ubiquitin-proteasome pathway. *Cell* **94,** 217–227
17. Arteaga, M. F., Wang, L., Ravid, T., Hochstrasser, M., and Canessa, C. M. (2006) An amphipathic helix targets serum and glucocorticoid-induced kinase 1 to the endoplasmic reticulum-associated ubiquitin-conjugation machinery. *Proc. Natl. Acad. Sci. U.S.A.* **103,** 11178–11183
18. Nakatsukasa, K., Huyer, G., Michaelis, S., and Brodsky, J. L. (2008) Dissecting the ER-associated degradation of a misfolded polytopic membrane protein. *Cell* **132,** 101–112
19. Ellgaard, L., and Helenius, A. (2003) Quality control in the endoplasmic reticulum. *Nat. Rev. Mol. Cell Biol.* **4,** 181–191
20. Ellgaard, L., Molinari, M., and Helenius, A. (1999) Setting the standards: quality control in the secretory pathway. *Science* **286,** 1882–1888
21. Kostova, Z., and Wolf, D. H. (2003) For whom the bell tolls: protein quality control of the endoplasmic reticulum and the ubiquitin-proteasome connection. *EMBO J.* **22,** 2309–2317
22. Hampton, R. Y., and Rine, J. (1994) Regulated degradation of HMG-CoA reductase, an integral membrane protein of the endoplasmic reticulum, in yeast. *J. Cell Biol.* **125,** 299–312
23. Jensen, T.J., Loo, M.A., Pind, S., Williams, D.B., Goldberg, A.L., and Riordan, J. R. (1995) Multiple proteolytic systems, including the proteasome, contribute to CFTR processing. *Cell* **83,** 129–135
24. Pariyarath, R., Wang, H., Aitchison, J. D., Ginsberg, H. N., Welch, W. J., Johnson, A. E., and Fisher, E. A. (2001) Co-translational interactions of apoprotein B with the ribosome and translocon during lipoprotein assembly or targeting to the proteasome. *J. Biol. Chem.* **276,** 541–550
25. Vembar, S. S., and Brodsky, J. L. (2008) One step at a time: endoplasmic reticulum-associated degradation. *Nat. Rev. Mol. Cell Biol.* **9,** 944–957
26. Marques, C., Pereira, P., Taylor, A., Liang, J. N., Reddy, V. N., Szweda, L. I., and Shang, F. (2004) Ubiquitin-dependent lysosomal degradation of the HNE-modified proteins in lens epithelial cells. *FASEB J.* **18,** 1424–1426
27. Guerriero, C. J., Weiberth, K. F., and Brodsky, J. L. (2013) Hsp70 targets a cytoplasmic quality control substrate to the San1p ubiquitin ligase. *J. Biol. Chem.* **288,** 18506–18520
28. Summers, D. W., Wolfe, K. J., Ren, H. Y., and Cyr, D. M. (2013) The type II Hsp40 Sis1 cooperates with Hsp70 and the E3 ligase Ubr1 to promote degradation of terminally misfolded cytosolic protein. *PLoS ONE* **8,** e52099
29. Sharma, D., and Masison, D. C. (2011) Single methyl group determines prion propagation and protein degradation activities of yeast heat shock protein (Hsp)-70 chaperones Ssa1p and Ssa2p. *Proc. Natl. Acad. Sci. U.S.A.* **108,** 13665–13670
30. Adle, D. J., and Lee, J. (2008) Expressional control of a cadmium-transporting P1B-type ATPase by a metal sensing degradation signal. *J. Biol. Chem.* **283,** 31460–31468
31. Adle, D. J., Sinani, D., Kim, H., and Lee, J. (2007) A cadmium-transporting P1B-type ATPase in yeast *Saccharomyces cerevisiae*. *J. Biol. Chem.* **282,** 947–955
32. Becker, J., Walter, W., Yan, W., and Craig, E. A. (1996) Functional interaction of cytosolic hsp70 and DnaJ-related protein, Ydjl, in protein translocation *in vivo*. *Mol. Cell. Biol.* **16,** 4378–4386
33. Mumberg, D., Müller, R., and Funk, M. (1995) Yeast vectors for the controlled expression of heterologous proteins in different genetic backgrounds. *Gene* **156,** 119–122
34. Ho, S. N., Hunt, H. D., Horton, R. M., Pullen, J. K., and Pease, L. R. (1989) Site-directed mutagenesis by overlap extension using the polymerase chain reaction. *Gene* **77,** 51–59
35. Smith, D. B., and Johnson, K. S. (1988) Single-step purification of polypeptides expressed in *Escherichia coli* as fusions with glutathione S-transferase. *Gene* **67,** 31–40
36. Ausubel, F. M., Brent, R., Kingston, R. E., Moore, D. D., Seidman, J. G., Smith, J. A., and Struhl, K. (1987) *Curr. Protoc. Mol. Biol.* Greene Publishing Associates and Wiley-Interscience, New York
37. Gietz, R. D., Schiestl, R. H., Willems, A. R., and Woods, R. A. (1995) Studies on the transformation of intact yeast cells by the LiAc/SS-DNA/PEG procedure. *Yeast* **11,** 355–360
38. Moxley, M. A., Sanyal, N., Krishnan, N., Tanner, J. J., and Becker, D. F. (2014) Evidence for hysteretic substrate channeling in the proline dehydrogenase and δ1-pyrroline-5-carboxylate dehydrogenase coupled reaction of proline utilization A (PutA). *J. Biol. Chem.* **289,** 3639–3651
39. Wei, W., Smith, N., Wu, X., Kim, H., Seravalli, J., Khalimonchuk, O., and Lee, J. (2014) YCF1-mediated cadmium resistance in yeast is dependent on copper metabolism and antioxidant enzymes. *Antioxid. Redox Signal.* **21,** 1475–1489
40. Jorgensen, P., Nishikawa, J. L., Breitkreutz, B. J., and Tyers, M. (2002) Systematic identification of pathways that couple cell growth and division in yeast. *Science* **297,** 395–400
41. McCullum, E. O., Williams, B. A., Zhang, J., and Chaput, J. C. (2010) Random mutagenesis by error-prone PCR. *Methods Mol. Biol.* **634,** 103–109
42. Singh, M. V., and Weil, P. (2002) A method for plasmid purification directly from yeast. *Anal. Biochem.* **307,** 13–17
43. Altschul, S. F., Gish, W., Miller, W., Myers, E. W., and Lipman, D. J. (1990) Basic local alignment search tool. *J. Mol. Biol.* **215,** 403–410
44. Thompson, J. D., Higgins, D. G., and Gibson, T. J. (1994) ClustalW: improving the sensitivity of progressive multiple sequence alignment through sequence weighting, position-specific gap penalties and weight matrix choice. *Nucleic Acids Res.* **22,** 4673–4680
45. Zhang, Y. (2008) I-TASSER server for protein 3D structure prediction. *BMC Bioinformatics* **9,** 40
46. Moriuchi, H., Moriuchi, M., Pichyangkura, R., Triezenberg, S. J., Straus, S. E., and Cohen, J. I. (1995) Hydrophobic cluster analysis predicts an amino-terminal domain of varicella zoster virus open reading frame 10 required for transcriptional activation. *Proc. Natl. Acad. Sci. U.S.A.* **92,** 9333–9337
47. Moulis, J. M. (2010) Cellular mechanisms of cadmium toxicity related to the homeostasis of essential metals. *Biometals* **23,** 877–896
48. Epping, E. A., and Moye-Rowley, W. S. (2002) Identification of interdependent signals required for anterograde traffic of the ATP-binding cassette transporter protein Yor1p. *J. Biol. Chem.* **277,** 34860–34869
49. Zhang, Y., Nijbroek, G., Sullivan, M. L., McCracken, A. A., Watkins, S. C., Michaelis, S., and Brodsky, J. L. (2001) Hsp70 molecular chaperone facilitates endoplasmic reticulum-associated protein degradation of cystic fibrosis transmembrane conductance regulator in yeast. *Mol. Biol. Cell* **12,** 1303–1314
50. Fürst, P., Hu, S., Hackett, R., and Hamer, D. (1988) Copper activates metallothionein gene transcription by altering the conformation of a specific DNA binding protein. *Cell* **55,** 705–717

51. He, L., Wang, B., Hay, E. B., and Nebert, D. W. (2009) Discovery of ZIP transporters that participate in cadmium damage to testis and kidney. *Toxicol. Appl. Pharmacol.* **238,** 250–257
52. Méplan, C., Mann, K., and Hainaut, P. (1999) Cadmium induces conformational modifications of wild-type p53 and suppresses p53 response to DNA damage in cultured cells. *J. Biol. Chem.* **274,** 31663–31670
53. Varshavsky, A. (1996) The N-end rule: functions, mysteries, uses. *Proc. Natl. Acad. Sci. U.S.A.* **93,** 12142–12149
54. Rechsteiner, M., and Rogers, S. W. (1996) PEST sequences and regulation by proteolysis. *Trends Biochem. Sci.* **21,** 267–271
55. Petäjä-Repo, U. E., Hogue, M., Bhalla, S., Laperrière, A., Morello, J. P., and Bouvier, M. (2002) Ligands act as pharmacological chaperones and increase the efficiency of δ opioid receptor maturation. *EMBO J.* **21,** 1628–1637
56. Tateishi, Y., Kawabe, Y., Chiba, T., Murata, S., Ichikawa, K., Murayama, A., Tanaka, K., Baba T., Kato, S., and Yanagisawa, J. (2004) Ligand-dependent switching of ubiquitin-proteasome pathways for estrogen receptor. *EMBO J.* **23,** 4813–4823
57. Hampton, R. Y., and Garza, R. M. (2009) Protein quality control as a strategy for cellular regulation: lessons from ubiquitin-mediated regulation of the sterol pathway. *Chem. Rev.* **109,** 1561–1574
58. Changela, A., Chen, K., Xue, Y., Holschen, J., Outten, C. E., O'Halloran, T. V., and Mondragón, A. (2003) Molecular basis of metal-ion selectivity and zeptomolar sensitivity by CueR. *Science* **301,** 1383–1387
59. Smith, N., Wei W., and Lee, J. (2013) Cadmium transport in eukaryotes in *Encyclopedia of Inorganic and Bioinorganic Chemistry* (Scott, R. A., ed.) pp. 1–12, John Wiley & Sons, Ltd., Chichester, UK
60. Heo, D. H., Baek, I. J., Kang, H. J., Kim, J. H., Chang, M., Kang, C. M., and Yun, C. W. (2012) Cd^{2+} binds to Atx1 and affects the physical interaction between Atx1 and Ccc2 in *Saccharomyces cerevisiae*. *Biotechnol. Lett.* **34,** 303–307
61. Giles, N. M., Watts, A. B., Giles, G. I., Fry, F. H., Littlechild, J. A., and Jacob, C. (2003) Metal and redox modulation of cysteine protein function. *Chem. Biol.* **10,** 677–693
62. Waldron, K. J., Rutherford, J. C., Ford, D., and Robinson, N. J. (2009) Metalloproteins and metal sensing. *Nature* **460,** 823–830
63. Mao, X., Kim, B. E., Wang, F., Eide, D. J., and Petris, M. J. (2007) A histidine-rich cluster mediates the ubiquitination and degradation of human zinc transporter, hZIP4, and protects against zinc cytotoxicity. *J. Biol. Chem.* **282,** 6992–7000
64. Smith, A. T., Smith, K. P., and Rosenzweig, A. C. (2014) Diversity of the metal-transporting P1B-type ATPases. *J. Biol. Inorg. Chem.* **19,** 947–960
65. Gilon, T., Chomsky, O., and Kulka, R. G. (1998) Degradation signals for ubiquitin system proteolysis in *Saccharomyces cerevisiae*. *EMBO J.* **17,** 2759–2766
66. Gilon, T., Chomsky, O., and Kulka, R. G. (2000) Degradation signals recognized by the Ubc6p-Ubc7p ubiquitin-conjugating enzyme pair. *Mol. Cell. Biol.* **20,** 7214–7219
67. Viana, R. J., Nunes, A. F., and Rodrigues, C.M. (2012) Endoplasmic reticulum enrollment in Alzheimer's disease. *Mol. Neurobiol.* **46,** 522–534
68. Mercado, G., Valdés, P., and Hetz, C. (2013) An ERcentric view of Parkinson's disease. *Trends Mol. Med.* **19,** 165–175
69. Brodsky, J. L. (2007) The protective and destructive roles played by molecular chaperones during ERAD (endoplasmic-reticulum-associated degradation). *Biochem. J.* **404,** 353–363
70. Lukacs, G. L., and Verkman, A. S. (2012) FTR: folding, misfolding and correcting the δF508 conformational defect. *Trends Mol. Med.* **18,** 81–91
71. Brown, C. R., Hong-Brown, L. Q., Biwersi, J., Verkman, A. S., and Welch, W. J. (1996) Chemical chaperones correct the mutant phenotype of the δ F508 cystic fibrosis transmembrane conductance regulator protein. *Cell Stress Chaperones* **1,** 117–125
72. Zhou, Z., Gong, Q., and January, C. T. (1999) Correction of defective protein trafficking of a mutant HERG potassium channel in human long QT syndrome: pharmacological and temperature effects. *J. Biol. Chem.* **274,** 31123–31126
73. Shearer, A. G., and Hampton, R. Y. (2004) Structural control of endoplasmic reticulum-associated degradation: effect of chemical chaperones on 3-hydroxy-3-methylglutaryl-CoA reductase. *J. Biol. Chem.* **279,** 188–196
74. Cortez, L., and Sim, V. (2014) The therapeutic potential of chemical chaperones in protein folding diseases. *Prion* **8,** 197–202, 10.4161/pri.28938